

Title:
**Design and Dispatch Optimization of Packaged Ice Storage Systems Within a Connected
Community**

Authors:

Karl Heine

Colorado School of Mines and National Renewable Energy Laboratory
ORCID: 0000-0003-2077-6634
Email: kheine@mines.edu

Paulo Cesar Tabares-Velasco*

Colorado School of Mines and National Renewable Energy Laboratory
ORCID: 0000-0001-5401-7594
Email: tabares@mines.edu
* Corresponding Author

Michael Deru

National Renewable Energy Laboratory
ORCID: 0000-0002-3179-1955
Email: michael.deru@nrel.gov

Title: Design and Dispatch Optimization of Packaged Ice Storage Systems within a Connected Community

Highlights

- A simulation-optimization workflow to design and dispatch packaged ice storage systems within a connected community is presented.
- The workflow is demonstrated on a seven-building case study with 17 rooftop air conditioning units using an existing electric utility rate.
- Accounting for storage hardware costs, annual cooling-only energy costs are reduced 17.8% with optimal design and dispatch.
- Community optimization provides different design and greater cost savings compared to optimizing each building individually.

Keywords

Connected community optimization

Cool thermal energy storage

Mixed-integer linear programming

Packaged ice storage

Unitary thermal storage systems

Energy storage

EnergyPlus

Abstract

The traditional implementation of cool thermal energy storage (CTES) must be reimagined within the context of a dynamic grid and smart buildings operating as connected communities. As most buildings do not operate central chillers or connect to district cooling loops, this necessitates a broader use of packaged CTES. Our objective is to begin answering the question of how such packaged CTES should be implemented within a connected community. We do so by presenting a simulation-optimization workflow employing building energy modeling software and a mixed-integer linear program to design and dispatch a packaged CTES technology to achieve minimum total annual cost. We demonstrate this methodology on a seven-

building case study using current utility rates and find that total annual cooling energy costs can be reduced by 17.8% compared to baseline, after accounting for the cost of storage. We perform three parametric sensitivity studies to evaluate modeling assumptions and obtain the prioritization of storage procurement as a function of annualized life-cycle cost of storage. We find that a community optimization approach provides significantly different results than individual building optimizations and provides greater savings compared to baseline.

Nomenclature

BEM	Building energy modeling
COP	Coefficient of performance
CTES	Cool thermal energy storage
GEB	Grid-interactive efficient buildings
MILP	Mixed-integer linear program
PSZAC	Packaged single zone air conditioner
PVAV	Packaged variable-air-volume
RTU	Rooftop unit
SOC	State-of-charge
TOU	Time-of-use
UTSS	Unitary thermal storage system

1. Introduction and Literature Review

The growth of renewable assets within energy generation portfolios across the U.S. is changing the paradigm that buildings are simple energy users [1]. Instead, the future grid requires interactive buildings with smart controls, that can coordinate with other buildings for the mutual benefit of the building occupants, facility owners, and utility providers. These grid-interactive efficient buildings (GEB) can provide electric load flexibility as a service to the grid [2]. One of the primary methods of providing this flexibility is through load shifting, in which a portion of the building's electricity use is temporally moved into off-peak hours or hours with excess renewable energy generation through the use of energy storage [3]. Considering the significant energy use by cooling equipment, especially during summer mid- to late-afternoon hours during which cooling drives electric peak demand, substantial electrical load shifting can often be performed using cool thermal energy storage (CTES) [4-7]. Furthermore, coordination between multiple buildings with diverse electricity profiles can provide greater value to the grid compared to controlling individual building loads in isolation [8]. A broad research question is implied: how *should* CTES be installed and operated in a GEB community to best support the

dynamic generation of the future grid? This paper presents a tool to help answer that question using the specific technology of packaged ice storage.

Centralized CTES, attached to main chiller plants, is a proven method for load shifting to obtain energy bill savings [9-11]. Under common commercial utility rates, centralized CTES consistently provides substantial electric demand reduction, and sometimes total energy use reduction [12]. Building energy simulation and parametric analyses have shown total plant operating cost reductions of 9-18.6%, and demand reduction during on-peak hours of 25-78% throughout the year [13-15]. Optimizations of ice storage using non-linear, linear, and mixed-integer programming [16-19], neural networks and genetic algorithms [20-22], and multi-objective approaches [23] have shown the potential to greatly reduce cooling energy costs – up to 25-30% in hot climates with high on-peak electric rates. These studies were performed on a mix of individual commercial buildings and district cooling loops. Chilled water storage is often economically preferable to ice at very large scales; however, ice thermal storage has been effectively implemented in district cooling systems [24, 25]. In the context of a dynamic grid, recent studies show how CTES in general, and ice thermal storage specifically, provide a grid service, such as reducing power generation costs [26] or facilitating renewable penetration and utilization [27, 28]. However, only 25% of commercial floorspace in the U.S. is cooled via central plants, while an estimated 66% of commercial floorspace is cooled by packaged rooftop units (RTU) [29]. It is this latter market category which offers the most aggregated potential for cooling load flexibility, but has not been well assessed in literature.

To address this growing need for thermal storage in distributed applications, recent research has focused on the development of unitary thermal storage systems (UTSS). These are self-contained cool thermal storage devices that can be readily integrated into a building's existing packaged cooling equipment, specifically RTUs [30]. While some technologies using various phase-change materials are under development [31, 32], only one ice-based system was commercially available in recent years [33, 34]. This system serves as the basis for a packaged ice storage model within the EnergyPlus building energy modeling (BEM) software [35, 36]. The charge and discharge performance for this packaged unit are described in [37]. We employ this UTSS performance regression model in this study, with additional discussion in §2.3 *UTSS Model* below.

Modeling and optimization of cooling systems as distributed energy resources (DERs) at the community scale is an area of active research and technological development. Several studies have shown that approaching energy flexibility at the community scale can provide greater potential than through an individual building approach [38-41]. New tools are available for assessing and optimizing thermal storage within the community context, both open-source [42, 43] and proprietary [44, 45]. However, none of these tools yet have the capability of modeling or optimizing ice-based UTSS at individual RTUs. Thus, the question of how beneficial such a technology might be to the GEB future remains unanswered.

The objective of this study is to address this research gap by developing a new workflow that optimizes the location and operation of unitary thermal storage systems (UTSS) as distributed energy resources (DERs) within a connected community. The contributions of this paper are: (1) a simulation-optimization workflow for evaluating unitary thermal storage systems (UTSS) as DERs; (2) a mixed-integer linear program (MILP) to procure and dispatch UTSS within a connected community; (3) a demonstration of the efficacy of this workflow and assessment of MILP sensitivity to three UTSS model parameters using a seven-building case study; and (4) an application of the MILP to show that community optimization of UTSS outperforms the aggregation of individual building optimizations.

2. Methodology

2.1 Overview of Simulation-Optimization Workflow

We present a simulation-optimization workflow that employs BEM and MILP optimization to design and dispatch packaged ice energy storage within a connected community. The workflow is modular and scalable, capable of simultaneously evaluating multiple thermal storage systems at scales ranging from a single building with one air conditioner to many buildings, each containing several RTUs. The workflow is intended to provide early-design insight into the optimal placement and control of distributed cool thermal storage under the GEB paradigm. Figure 1 depicts the workflow, illustrating the required building energy, ice storage, and mathematical optimization models (blue), input data sets (white), simulation and optimization processes (orange), and final output results (green). There are three distinct phases of the workflow described below:

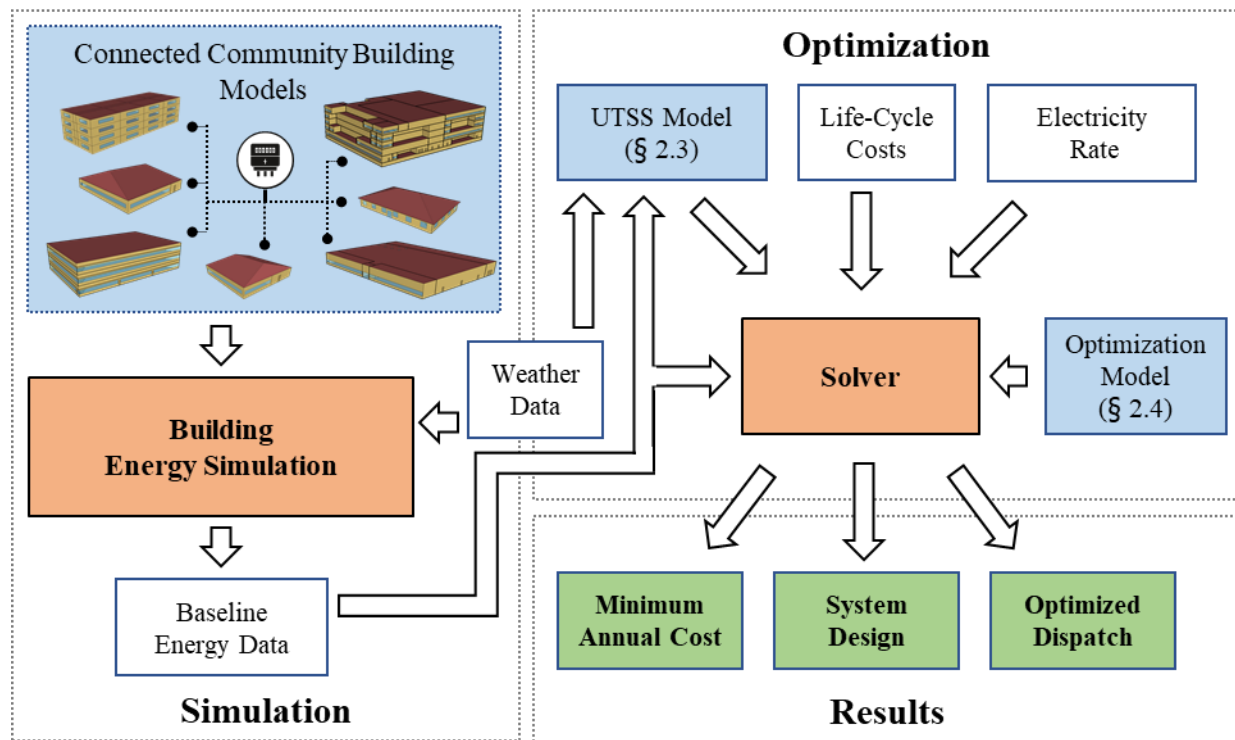


Figure 1: A simulation-optimization workflow to design and dispatch packaged thermal storage systems in a connected community of grid-interactive buildings. Background colors designate element type: blue for models, white for input data sets, orange for simulation and optimization processes, and green for final results. Section numbers indicate where the UTSS and optimization models are presented in this paper.

- The **Simulation phase** requires building energy models and weather data. The results of the BEM are the baseline energy use for all buildings and specific data at each RTU cooling system for every simulation timestep. These data become inputs for both the packaged ice storage model and the optimization program.
- The **Optimization phase** of the workflow requires the pre-processed parameters from the baseline energy data, the packaged ice storage model results, life-cycle cost data, and the electric utility rate. The packaged ice storage model is a stand-alone Python script that uses baseline building energy data and weather data to calculate charging and discharging capacities and efficiencies for the packaged ice storage system at each timestep and potential installation site within the community. This model and its assumptions are described in §2.3 *UTSS Model*. The life-cycle cost estimate for the packaged ice storage must be scaled to the optimization time horizon. To capture the seasonality of energy use, we examine a 12-month window and calculate the cost of storage using an annualized life-cycle cost (ALCC). The ALCC includes initial capital and installation costs, government

and utility incentives, annual device maintenance, and end-of-life costs, annualized over the expected lifespan of the device. Electricity rate information is the final input required for the optimization. Any combination of variable time-of-use energy and/or demand charges may be used, though complex tiered electricity rates may require constraint reformulation.

- The **Results phase** post-processes the optimization outputs for (1) minimum annual cost, (2) distributed packaged storage system design, and (3) the optimized dispatch, into user-friendly visualizations. In assessing these results, we determine the load shift efficiency (η_{shift}) of the optimized system, calculated relative to the total baseline energy use for the community. It is equal to the ratio of the electric load reduction from ice discharging (Load Shed) and the electric load increase from ice charging (Load Add), given by Equation 1 (see Table 1 for notation). Because this metric is highly sensitive to operating conditions and dispatch strategy, it is useful for comparing thermal storage design and control options.

$$\eta_{shift} = \frac{\text{Load Shed}}{\text{Load Add}} = \frac{\sum_{\{t|P_t < \hat{p}_t\}} P_t}{\sum_{\{t|P_t \geq \hat{p}_t\}} P_t} \quad (1)$$

2.2 Notation

To keep the mathematical expressions required by the UTSS model and the optimization formulation as short as possible, single-character symbols are preferred, except where such might cause confusion. Table 1 defines all notation used in both the packaged ice storage model and the optimization program formulation. For brevity, we use the UTSS acronym to refer to packaged ice storage systems for the remainder of this paper. Generally, parameters are designated with lower-case symbols and optimization variables are uppercase, except for temperature (T), heat transfer coefficient (UA), and coefficient of performance (COP). Superscripts provide descriptors and subscripts are reserved for indexing. Sets are also capitalized but are differentiated from variables with script font.

Table 1: Notation for UTSS model and optimization program

<i>Sets</i>	
$i \in \mathbf{I}$	Set of available UTSS types
$d \in \mathbf{D}$	Set of utility demand periods in the optimization horizon
$n \in \mathbf{N}$	Set of RTUs within the community
$t \in \mathbf{T}$	Set of all timesteps within the optimization period
$t \in \mathbf{T}_d^p$	Indexed set of timesteps within each utility demand period d
$t \in \mathbf{T}_n^l$	Indexed set of timesteps during which cooling load exists at RTU n
<i>Building Simulation Parameters</i>	
COP_{nt}^N	Coefficient of performance for RTU n at time t [kW_t/kW_e]
l_{nt}	Thermal cooling load served by RTU n at time t [kW_t]
\tilde{p}_t	Aggregated average power for the community at time t [kW_e]
T_t^d	Ambient dry-bulb temperature at time t [$^\circ\text{C}$]
T_{nt}^w	Wet-bulb temperature at the inlet to RTU n at time t [$^\circ\text{C}$]
<i>UTSS Parameters</i>	
$\dot{\alpha}_{it}$	Discharge effectiveness of UTSS type i at RTU n and time t [-]
$\tilde{\alpha}_i$	Nominal discharge effectiveness of UTSS type i [-]
η_{it}^S	Thermal storage tank efficiency for UTSS type i at time t [-]
$COP_i^{X,nom}$	Nominal Coefficient of performance for charging of UTSS i [kW_t/kW_e]
COP_{it}^X	Coefficient of performance of charging for UTSS type i at time t [kW_t/kW_e]
$COP_i^{Y,nom}$	Nominal Coefficient of performance for discharging of UTSS i [kW_t/kW_e]
COP_{it}^Y	Coefficient of performance for discharging UTSS type i at time t [kW_t/kW_e]
\bar{q}_i	Maximum thermal storage capacity of UTSS type i [kWh_t]
$\dot{q}_i^{X,nom}$	Nominal rate of charging of UTSS type i at time t [kW_t]
\dot{q}_{it}^X	Maximum rate of charging of UTSS type i at time t [kW_t]
$\dot{q}_i^{Y,nom}$	Nominal rate of discharging of UTSS type i at time t [kW_t]
\dot{q}_{it}^Y	Maximum rate of discharging of UTSS type i at time t [kW_t]
\tilde{s}_i	Constant for approximate median state-of-charge for UTSS type i [-]
T_i^{fz}	Freezing temperature of the thermal storage medium in UTSS type i [$^\circ\text{C}$]
UA_i	Net tank heat transfer coefficient times surface area for UTSS type i [$\text{kW}_t/^\circ\text{C}$]
<i>Cost Parameters</i>	
c_t^e	Cost of electric energy at time t [$\$/\text{kWh}_e$]
c_d^p	Cost of maximum average electric power during period d [$\$/\text{kW}_e$]

k_{in}	Annualized life cycle cost of storage for UTSS type i at RTU n [$\$/\text{device-year}$]
<i>Miscellaneous Parameters</i>	
δ	Duration of each timestep t [hr]
m_{in}	Maximum number of UTSS type i that may be installed at RTU n [-]
S_{in}^0	Initial thermal storage inventory for UTSS type i at RTU n [kW_t]
<i>Integer Variables</i>	
Z_{in}	Number of UTSS type i installed at RTU n [-]
<i>Continuous Variables</i>	
\hat{P}_d	Maximum aggregated power during period d [kW_e]
P_t	Total aggregated power at time t [kW_e]
S_{int}	Thermal storage energy inventory for UTSS type i at RTU n at time t [kWh_t]
X_{int}	Average thermal load added (charged) by UTSS type i at RTU n at time t [kW_t]
Y_{int}	Average thermal load reduced (discharged) by UTSS type i at RTU n at time t [kW_t]

2.3 UTSS Model

Figure 2 provides a general sketch of how a UTSS interacts with existing building cooling equipment. The selected UTSS integrates a packaged thermal storage unit – containing an ice storage tank, ice-making equipment, and refrigerant management system – with the air-conditioning equipment in a roof-top unit (RTU).

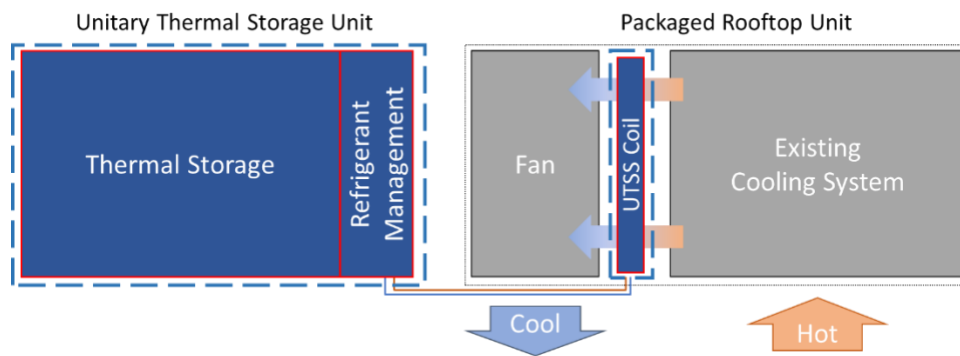


Figure 2: Depiction of a UTSS integrated with an RTU. Components of the UTSS are shown in blue. Note the placement of the UTSS evaporator coil within the RTU airstream [46].

The UTSS model is based on a set of non-linear performance curves found in the EnergyPlus Coil:Cooling:DX:SingleSpeed:ThermalStorage model object [35, 36] with additional detail provided in [37]. From this BEM object, we extract the performance curves and place them into an external Python script, to allow for workflow modularity and independence

from any specific BEM software. The coefficients used in Equations 2-4 are based on the IceBear 30, formerly manufactured by Ice Energy Inc., and included with the EnergyPlus UTSS model [35].

The UTSS model outputs five parameter sets required by the optimization program: maximum rate of thermal storage discharging (\dot{q}_{it}^Y), maximum rate of thermal storage charging (\dot{q}_{it}^X), coefficient of performance for charging (COP_{it}^X), discharge effectiveness ($\dot{\phi}_{int}$), and the tank thermal storage efficiency (η_{it}^S). These parameters are calculated using Equations 2-4, where the index of the UTSS type (i) is set equal to 1, since the coefficients are unique to our UTSS model.

Equation 2 calculates the maximum rate of discharging (\dot{q}_{it}^Y) as a function of nominal discharging rate and the wet-bulb temperature at the inlet of each roof-top unit (T_{nt}^w). Because each RTU has a different mix of return air from the building and fresh outside air, the inlet wet-bulb temperatures for each RTU at each timestep are obtained from the building energy simulation results, rather than from the ambient conditions in the weather file.

$$\dot{q}_{int}^Y = \dot{q}_1^{Y,nom} \left(-0.002765 \cdot (T_{nt}^w)^2 + 0.133949 \cdot T_{nt}^w - 0.561476 \right) \quad (2)$$

The maximum rate of charge is modeled as a function of nominal charging rate, tank state-of-charge (SOC), and ambient dry-bulb temperature (T_t^d). However, to retain a linear formulation, the timestep variation of state-of-charge must be eliminated. For a fixed dry-bulb temperature, the maximum rate of charging varies $\pm 7\%$ from the nominal rate as SOC fluctuates between 5% and 95%. Maximum charging rate decreases with SOC due to the growth of ice around the heat exchange coils within the tank, which slows the rate of heat transfer into storage. Rather than derive an approximate linearization of this relationship, we introduce a fixed parameter and set it equal to an expected value for the median state-of-charge of the ice tank (\tilde{s}_i). We examine the validity of this assumption and the optimization sensitivity to this parameter in §4.4 *Sensitivity Results*. The simplified curve, which assumes a median state-of-charge greater than 0.15, is given in Equation 3:

$$\dot{q}_{it}^X = \dot{q}_1^{X,nom} \left(1.293 - 0.127 \cdot \tilde{s}_1 + 0.0186 \cdot \tilde{s}_1^2 - 0.0083 \cdot T_t^d - 0.0001 \cdot (T_t^d)^2 + 0.0013 \cdot \tilde{s}_1 \cdot T_t^d \right) \quad (3)$$

Equation 4 calculates coefficient of performance (COP) when UTSS is making ice (charging) as a function of nominal COP, tank SOC, and T_t^d . The value of COP_{it}^X varies by \pm

3% with SOC values between 5% and 95%. As in the \dot{q}_{it}^X equation, we replace the timestep-varying SOC with an assumed median state-of-charge (\tilde{s}_1) for calculation of optimization parameters.

$$COP_{it}^X = \frac{COP_1^{X,nom}}{0.6208 + 0.0211 \cdot \tilde{s}_1 - 0.0015 \cdot \tilde{s}_1^2 - 0.0026 \cdot T_i^d + 0.0007 \cdot (T_i^d)^2 + 0.0018 \cdot \tilde{s}_1 \cdot T_i^d} \quad (4)$$

UTSS discharging COP is high (~ 63.9), since the compressor is off and only a small refrigerant circulation pump operates to provide cooling to the airstream. Our method combines RTU efficiency (COP_{nt}^N) and UTSS discharging efficiency (COP_{it}^Y) into a single discharge effectiveness value ($\tilde{\eta}$) for each RTU in Equation 5. We find this term more easily conceptualized than extremely high COPs that are not readily comparable to nominal RTU values. For example, if this UTSS were added to an ultra-high-efficiency RTU with a nominal COP of 4.4 (15 EER), the discharge effectiveness would be 93.1%. However, with a standard efficiency RTU having a COP of 3.23 (11 EER), the discharge effectiveness increases to 94.9%. If sufficient fidelity in the UTSS model is possessed, discharge effectiveness may be calculated at each RTU and timestep ($\dot{\eta}_{int}$) according to the general form of Equation 4. Because our model does not contain a performance curve for discharge efficiency, we assume a nominal value for discharge effectiveness ($\tilde{\eta}$).

$$\dot{\eta}_{int} = 1 - \left(\frac{COP_{nt}^N}{COP_{it}^Y} \right) \approx \tilde{\eta} \quad (5)$$

Equation 6 defines the UTSS tank efficiency at each timestep as a function of T_i^d , heat transfer coefficient and surface area (UA_i), tank freezing temperature (T_i^{fz}), optimization timestep (δ), and maximum UTSS storage capacity (\bar{q}_i). Losses through each thermal storage tank (η_{it}^s) are relatively small, with approximately 5% capacity loss over a summer day.

$$\eta_{it}^s = 1 - \frac{\delta \cdot UA_i \cdot (T_i^d - T_i^{fz})}{\bar{q}_i} \quad (6)$$

2.4 Distributed Storage Optimization Program

2.4.1 Objective Function

Our optimization program provides both procurement and placement of UTSS within the community (design) and charge/discharge control signals (dispatch) over the course of the year. The formulation is a mixed-integer linear program (MILP) consisting of twelve equation sets (Equation 7 and Constraints 8-18). The linear program ensures tractability and reasonable solution times when many buildings are simultaneously evaluated, and is similar to other strategic-level DER design-dispatch optimization tools [42, 47]. The objective function of the formulation minimizes total annual cost consisting of energy costs, demand charges, and the total annualized cost of storage, given by Equation 7.

$$\min \left[\sum_{t \in T} c_t^e (\delta \cdot P_t) + \sum_{d \in D} c_d^p \hat{P}_d + \sum_{i \in I} \sum_{n \in N} k_m Z_{in} \right] \quad (7)$$

2.4.2 Constraints

Constraint 8 is the heart of this formulation and calculates the optimal power for the community at each timestep (P_t) after applying thermal storage dispatch. It converts the linear decision variables (X_{int}, Y_{int}) for thermal load (in kW_t), used to charge or discharge individual UTSS devices, respectively, into deviations from the baseline community power draw (\tilde{p}_t) at each timestep t . To accomplish this, each decision variable is divided by the appropriate efficiency parameter. Dividing the thermal energy added from ice charging (X_{int}) is COP_{it}^X , provided by the UTSS model during pre-processing. The thermal energy reduced by discharging (Y_{int}) is similarly divided by a COP; however, this value is from the RTU at which storage is placed and is obtained from the building energy simulation results (COP_{nt}^N). The term is further modified by the nominal discharge effectiveness (\tilde{q}) which accounts for the small amount of electric energy used to discharge the thermal storage. The complete Y_{int} term represents the electrical power avoided at a given RTU and timestep by discharging the UTSS. The full constraint is written such that charging may occur at any timestep, but discharging can only occur if a thermal load is present at a given RTU. Constraint 9 then captures the maximum power during each demand period d .

$$P_t = \tilde{p}_t + \sum_{i \in I} \sum_{n \in N} \left[\frac{X_{int}}{COP_{it}^X} - \begin{cases} \frac{\tilde{\alpha}_t Y_{int}}{COP_{nt}^N} & \text{if } t \in T_n^l \\ 0 & \text{otherwise} \end{cases} \right] \quad \forall t \in T \quad (8)$$

$$\hat{P}_d \geq P_t \quad \forall d, t \in T_d^p \quad (9)$$

Constraints 10-12 limit the performance of each UTSS during discharging. The total load reduced by discharging cannot exceed: (1) the cooling demand from the building at that RTU (l_{nt}), given by Constraint 10; (2) the aggregated maximum rate of discharge of all the UTSS installed at each RTU, given by Constraint 11; and (3) the total available ice inventory at a given timestep (S_{int}), given by Constraint 12.

$$\sum_{i \in I} Y_{int} \leq l_{nt} \quad \forall n \in N, t \in T_n^l \quad (10)$$

$$Y_{int} \leq \dot{q}_{it}^Y \cdot Z_{in} \quad \forall i \in I, n \in N, t \in T_n^l \quad (11)$$

$$\delta \cdot Y_{int} \leq S_{int} \quad \forall i \in I, n \in N, t \in T_n^l \quad (12)$$

Constraint 13 limits the UTSS charging rate to be less than the aggregate maximum rate of charging for all UTSS installed at each RTU. Other restrictions on charging are provided by the inventory constraints.

$$X_{int} \leq \dot{q}_{it}^X \cdot Z_{in} \quad \forall i \in I, n \in N, t \in T \quad (13)$$

Thermal storage inventory (S_{int}) is initialized by Constraint 14 and limited to the maximum nominal storage capacity of each tank by Constraint 15. Constraints 16a and 16b provide inventory balance during the applicable timesteps. Because the decision variables are in units of kW_t, the optimization timestep δ is used to convert all terms into units of energy. Energy losses due to heat transfer between the tank and ambient are applied to each previous timestep's final state-of-charge.

$$S_{in1} = S_{in}^0 \quad \forall i \in I, n \in N \quad (14)$$

$$S_{int} \leq \bar{q}_i \cdot Z_{in} \quad \forall i \in I, n \in N, t \in T \quad (15)$$

$$S_{int} = \eta_{it}^S \cdot S_{in,t-1} + \delta \cdot X_{in,t-1} - \delta \cdot Y_{in,t-1} \quad \forall i \in I, n \in N, t > 1 \& \in T_n^l \quad (16a)$$

$$S_{int} = \eta_{it}^S \cdot S_{in,t-1} + \delta \cdot X_{in,t-1} \quad \forall i \in I, n \in N, t > 1 \& \notin T_n^l \quad (16b)$$

Constraints 17 and 18 ensure integrality and non-negativity. The number of UTSS units permitted at a given RTU is restricted by the parameter m_{in} , and is determined by physical system limitations.

$$X_{int}, Y_{int}, S_{int}, P_t, \hat{P}_d \geq 0 \quad \forall \quad i \in I, n \in N, t \in T, t' \in T_n^I, d \in D \quad (17)$$

$$0 \leq Z_{in} \leq m_{in}, \text{integer} \quad \forall \quad i \in I, n \in N \quad (18)$$

2.5 Limitations of this Approach

There are four main limitations to our approach:

1. *Median ice tank state-of-charge assumption.* The first and most notable limitation to our approach is the UTSS model's independence of time-varying SOC. In reality, UTSS efficiency and maximum rate of heat transfer are functions of both ambient conditions and SOC. However, inclusion of the SOC dependency in the optimization requires a non-linear formulation. For our UTSS Model, we assume a fixed parameter for median state of charge (\tilde{s}_1) to maintain a linear optimization formulation, which helps maintain tractability, especially for community-scale problems. The quality of this assumption is examined in §4.4 *Sensitivity Results*.
2. *Fixed-speed compressor assumption.* The second limitation of our approach is that we assume that a fraction of the cooling load can be subtracted from a specific air conditioning unit at a given timestep without affecting the baseline RTU efficiency. This assumption is valid only if the RTU in question uses a fixed-speed compressor. If so, part-load operation is achieved through equipment cycling and efficiency is only a function of air properties, which are treated as constants during a given timestep. If multi-stage compressors are used in the building models, our approach and formulation can still be applied, but efficiency changes between compressor stages will be neglected. To provide the most conservative estimate of UTSS performance, the highest efficiency stage should be used when calculating COP_{in}^N parameters.
3. *Unchanged zone loads assumption.* The third limitation of our approach is that we do not account for the variation in zone air conditions that would occur when using UTSS compared to the baseline building cooling systems. Because UTSS discharge on a variable continuum to meet the cooling load, they will typically run continuously at part-

load rather than frequently cycling. This will result in much more consistent dehumidification of the supply air compared to a direct-expansion air-conditioning unit, which in turn will affect the zone cooling loads over time. While this will affect cooling equipment energy use, it is unlikely to affect the optimization dispatch since it will result in a generally consistent change in zone air humidity for the full simulation period – there will be little, if any, differentiation between adjacent timesteps that would alter dispatching. If possible, this effect should be explored through re-simulation of the building models in BEM software. Such analysis is beyond the scope of this study.

4. *No explicit accounting for changes in fan energy use.* The final limitation of our approach is a lack of explicit accounting for the increased fan energy use when adding UTSS to the airstream. Each cooling coil adds approximately 0.1 in. of water (25 Pa) in pressure drop to the airflow [48]. This addition is relatively small compared to other airstream components, such as air filters or fan system effects; but it will be felt for the entire life of the system and should not be neglected from final energy calculations. To accurately capture this effect, additional fan information is required. Such analysis is beyond the scope of this study.

3. Case Study Community

3.1 Building Models and Location

Our workflow is demonstrated using a community that consists of seven simulated buildings located in El Paso, TX, which lies within ASHRAE Climate Zone 3B (Warm-Dry). This location has significant seasonal and diurnal temperature variation resulting in large variability in cooling loads over the course of the year. Typical meteorological year weather data for El Paso International Airport is used [49] and the building models are generated using an OpenStudio measure that creates prototype commercial buildings [50-52]. We simulate these buildings using EnergyPlus v.9.3 using a timestep of 1 minute, which is the maximum fidelity of the software. HVAC system types are either packaged single zone air conditioners (PSZAC) or packaged variable-air-volume (PVAV) systems. Table 2 lists the seven buildings used in this case study, summarizing their ASHRAE Standard 90.1 vintage, HVAC system type, number of RTUs, and the maximum building occupancy.

Table 2: Summary of connected community building models

Building Type	Standard 90.1 Vintage	HVAC Type	No. RTU's	Max Occ.
Fast Food	2010	PSZAC	2	94
Midrise Apartment	Pre-2004	PVAV	3	79
Medium Office	2007	PVAV	3	286
Small Office	2013	PVAV	1	31
Outpatient	2010	PVAV	2	419
Restaurant	2004	PSZAC	2	287
Retail	Pre-2004	PSZAC	4	371
Totals	-	-	17	1,567

Figure 3 shows the weighted occupancy of the entire community over a summer weekday. Community aggregate occupancy peaks at 14:00 and remains above 50% until after 20:00.

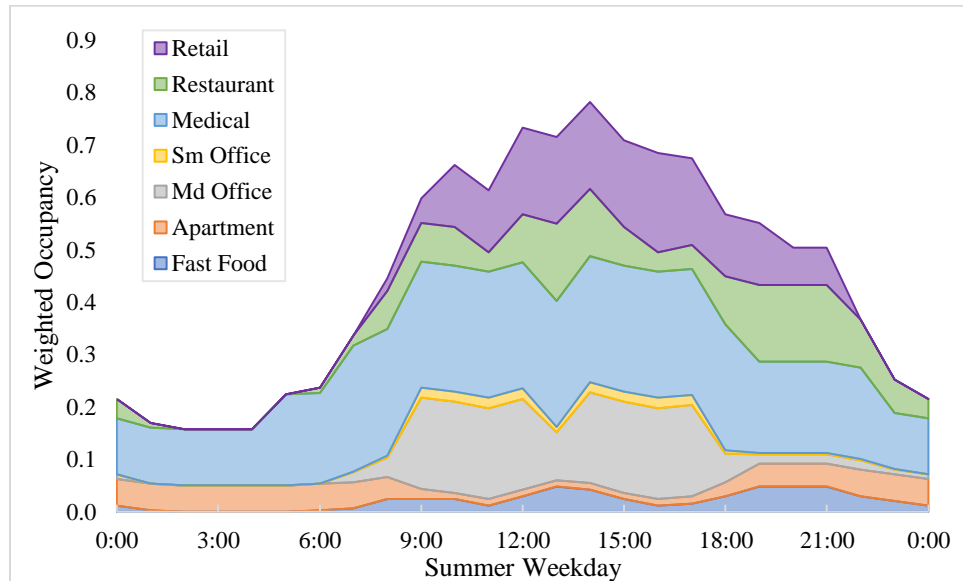


Figure 3: Aggregated weighted occupancies of each building type, presented to illustrate the temporal coincidence of building occupancy and relative sizes of each building.

Table 3 lists the total annual electricity use and cooling-only electricity use for each building. The fraction of total annual electricity used for cooling ranges between 8.8% and 24.0% for individual buildings and is 17.2% for the entire community. Figure 4 shows the 15-minute-averaged aggregated load profiles for (a) total power demand and (b) cooling-only power demand for each building over a peak day in June. While the peak community occupancy occurs at 14:00, on this day the maximum cooling-only power demand occurs at 14:45 and total power

demand peaks at 15:45. The fraction of total community power demand due to cooling loads on this day is 40%.

Table 3: Baseline building energy results

Building Type	Annual Cooling Electricity [MWh]	Annual Total Electricity [MWh]
Fast Food	14.1	159.9
Midrise Apartment	75.9	316.2
Medium Office	128.3	648.7
Small Office	6.4	44.3
Outpatient	234.6	1,243.9
Restaurant	46.9	401.5
Retail	72.7	554.0
Totals	578.9	3,368.5

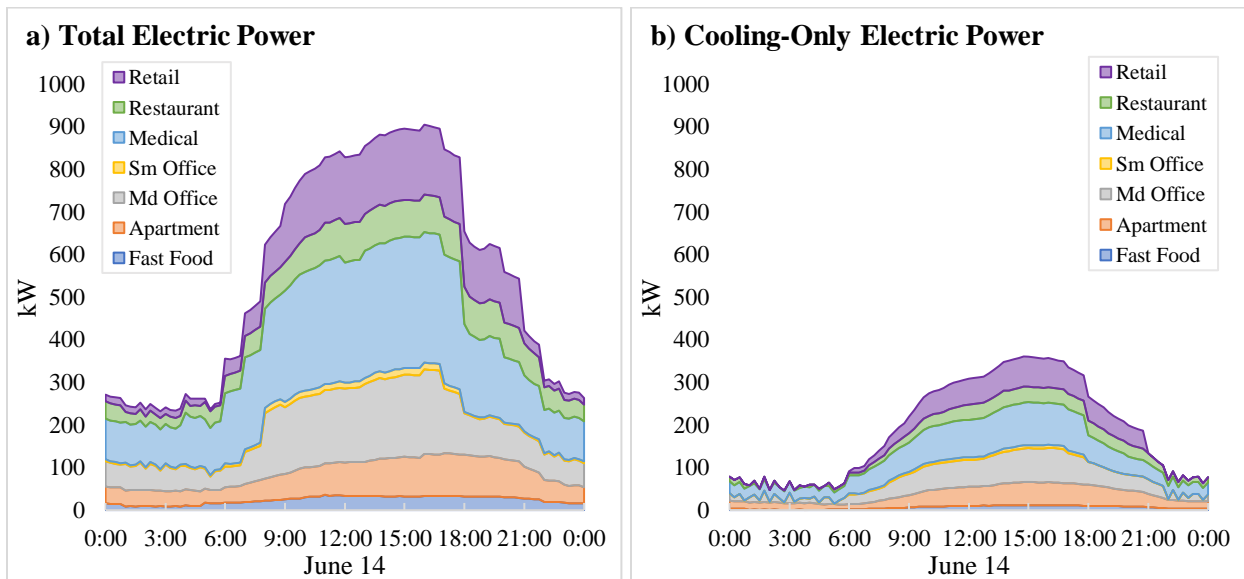


Figure 4: Aggregated electric power demand over a near-peak summer day from the baseline energy results: (a) total electric power demand; (b) cooling-only electric power demand.

We use the 2018 Large Power Service Rate (Schedule No. 25), from the El Paso Electric Company [53] as the reference electric rate for this case study. The rate includes seasonally varying monthly demand charges, assessed on the maximum 15-minute average, and time-of-use (TOU) energy charges. Demand charges are \$22.49 per kW_e during summer months (June-September) and \$18.36 per kW_e during winter (October-May). Time-of-use energy charges are \$0.11527 per kWh_e during on-peak and \$0.00502 per kWh_e during off-peak. On-peak hours are 12:00-18:00 throughout the summer months. Winter energy rates are a flat \$0.00502 per kWh_e. We ignore all fixed connection charges and do not apply special rules for holidays.

3.2 UTSS Model Data

In anticipation of new technologies, our optimization formulation is designed to handle multiple types of UTSS; however, this demonstration only evaluates one 40 ton-hour device formerly manufactured by Ice Energy [54, 55]. This device is well characterized through its limited market presence and has demonstrated both building-scale and grid-scale load-shifting capabilities [33]. Table 4 lists its nominal performance characteristics, as well as the constants used in optimization parameter calculations.

Table 4: Performance characteristics for the selected UTSS (index $i = 1$)

Parameter	Value	Remarks
\tilde{q}_1	0.93	Assumes high-efficiency RTU
$COP_1^{X,nom}$	3.09	Rated COP of charging
$COP_1^{Y,nom}$	63.9	Rated COP of discharging
\bar{q}_1	133.6 kW _t	95% of 40 ton-hours
$\dot{q}_1^{X,nom}$	17.6 kW _t	5-tons cooling for ice-making
$\dot{q}_1^{Y,nom}$	35.2 kW _t	10-tons cooling via ice discharge
\tilde{s}_1	0.55	Anticipated median tank state-of-charge
S_{1n}^0	0 kW _t	All ice tanks are initially fully discharged
T_1^{fz}	0°C	Freezing temperature of ice tank
UA_1	0.007913 kW _t /°C	Thermal loss rate as a function of temperature difference

3.3 Annualized Life Cycle Cost Estimate

The element of this analysis with the most uncertainty is the annualized life cycle cost (ALCC) of the UTSS unit. We use various sources [48, 56, 57] to obtain a realistic approximation for ALCC, itemized in Table 5. To address the uncertainty related to storage costs, we perform a parametric sweep over a broad range of possible ALCC values, discussed in §4.4 Sensitivity Results.

Table 5: Cost components used in estimating the annualized life cycle cost

Cost Component	Value Used	Remarks
UTSS Device	\$17,500 [48, 56]	-
Installation	\$10,000 [48, 56]	-
Permitting/Engineering	\$2,500 [48, 56]	Cost shared with RTU retrofit
New HVAC	Not Included	-
Incentive	(\$12,500) [48, 57]	Government and utility incentives
Tax Credit	Not Included	20-30% + accelerated depreciation ^[48]

End-of-Life	Not Included	Included w/installation above
Life-Cycle Cost	\$17,500	-
Service Life	20 years ^[48]	-
Annual Maintenance	\$250 per year ^[48]	Includes major service at 10 years
Annualized Life Cycle Cost	\$1,125 per year	

3.4 Solution Method and Sensitivity Analyses

This case study is solved using IBM CPLEX v. 12.10.0.0 on an Intel Xeon E5440 2.83GHz dual Quad-core machine with 16 GB of RAM, operating Ubuntu 18.04.5 LTS. Due to large number of continuous variables (~1.27 million after pre-solve) and small number of general integer variables (17), this formulation is well suited to use Benders Decomposition [58], which we employ using the built-in ‘benderopt’ solver option [59]. Further improvement in solution time is achieved with symmetry elimination on the COP_{it}^X parameter values (via $\leq 0.05\%$ perturbations), which we apply when reading the data into A Mathematical Programming Language (AMPL), the software used for MILP formulation and execution. Three small parametric analyses are performed to examine the program sensitivity to the UTSS model and formulation assumptions for the following parameters: \tilde{s}_1 , δ , and k_{in} .

To assess the potential impact of our assumed median UTSS state-of-charge (\tilde{s}_1) on the optimization results, we execute the full workflow using three different values for \tilde{s}_1 : 0.05, 0.55, and 0.95. When the ice tank is nearly empty, the contents are mostly water and the heat transfer rates are much higher than when the tank is mostly solidified into ice. More conservative UTSS performance estimates will be obtained at higher \tilde{s}_1 values. By bounding the UTSS at the near maximum and minimum states-of-charge, we quantify the potential significance of the \tilde{s}_1 assumption.

The timesteps used for building energy simulation and optimization do not need to match, so long as the optimization timestep is an integer multiple of the simulation timestep. Because building power demand is billed over a rolling 15-minute horizon, we consider this the required optimization timestep ($\delta = 0.25$ hours). However, previous literature has shown that modeling timestep can have a significant impact on calculated peak demand and the associated optimization results [60, 61]. By separating our building simulation process from the optimization, we take advantage of the highest available resolution in the energy modeling software (1-minute), but then apply the optimization over the 15-minute billing window used by

many utilities. To explore the impact of longer optimization timesteps, we average the 1-minute building energy simulation data over 15, 30, and 60-minute windows ($\delta = 0.25, 0.5, \text{ and } 1.0$) and evaluate the impact on the optimal solution. Shorter optimization timesteps result in exceedingly large matrices when performing full-year, multi-building analyses, and are not examined in this study.

As noted, the ALCC (k_{in}) is the most ambiguous element of the case study. To address this uncertainty, we iteratively solve the optimization using progressively increasing values for ALCC. We begin with a minimum k_{in} of \$50 per UTSS per year, which makes the thermal storage essentially free to procure and operate. We then increment the value of k_{in} by \$50 and re-solve, repeating the process until we reach the point where the UTSS cost becomes prohibitive, and the optimized solution returns no thermal storage.

4. Results and Discussion

4.1 Minimum Annual Cost

The optimization model solved in ~1.3 hours to a minimum annual cost of \$234,980 with 21 UTSS distributed across 11 of the 17 RTUs in five of the seven buildings. This provides \$12,420 in annual savings relative to the baseline community electric bill, which equates to a 4.9% annual savings in total electricity costs and a 17.8% savings in cooling-only electricity costs – even after accounting for the added \$23,625 in annual UTSS expenses. Figure 5 provides cost comparison between the optimal result and the baseline for (a) total electric and (b) cooling-only electric costs. The left columns on each plot are the sum of the remaining three cost components illustrated. While most savings are found in the reduction in demand charges, the optimization provides similar relative reductions for both energy and demand charges. Total energy charges are reduced 13.8% while demand charges are reduced by 14.8%. The energy and demand charges associated with cooling-only are reduced 45.2% and 54.4%, respectively.

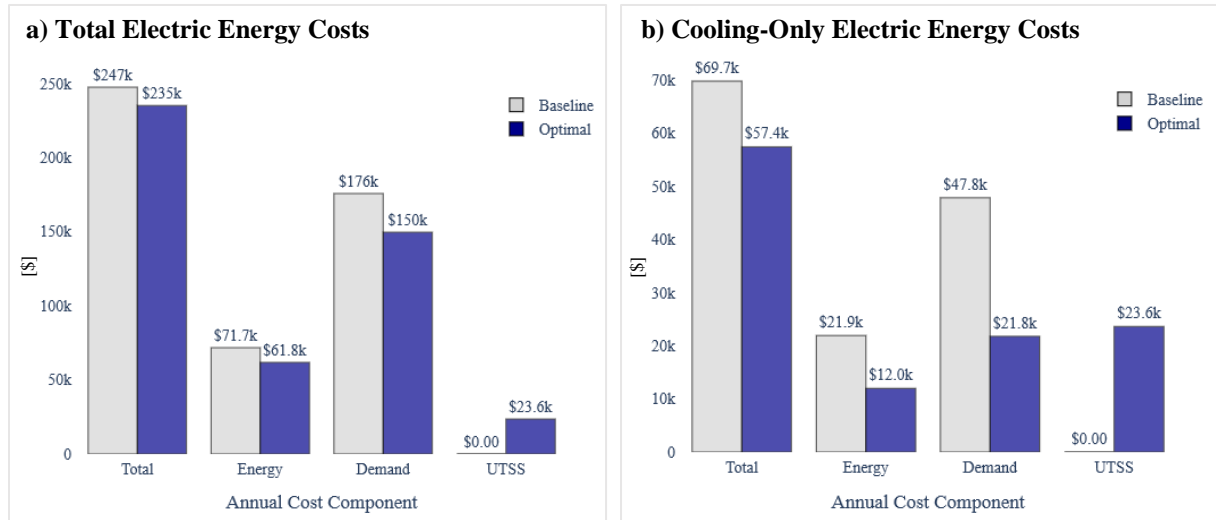


Figure 5: Cost comparison of the optimization program solution with baseline community energy bill. The total annual cost is the sum of the energy charges, demand charges, and ALCC for (a) [community aggregate] total electric energy costs and (b) cooling-only electric energy costs.

4.2 System Design

The distribution of the 21 UTSS across the community is illustrated by Figure 6, where the gray bars indicate the maximum number of UTSS that can potentially be installed at a given RTU (equal to the parameter m_m), determined in pre-processing from the nominal capacities of each RTU. The blue bars are the number of UTSS installed at a given RTU. Because there was little cooling load diversity in our case study, the results generally conform to expectations, with more UTSS assigned to larger RTUs. However, not all results are intuitive. For example, RTU 17 receives thermal storage while RTU 14 does not, despite being smaller. RTU 11, which is by far the largest unit within the entire community, receives the same number of thermal storage devices as the much smaller RTU 15. The value of thermal storage is not determined solely by the magnitude of the cooling load that can be shifted at a given RTU, but also by how that load coincides with other electricity power demand across the community, and by the utility tariff.

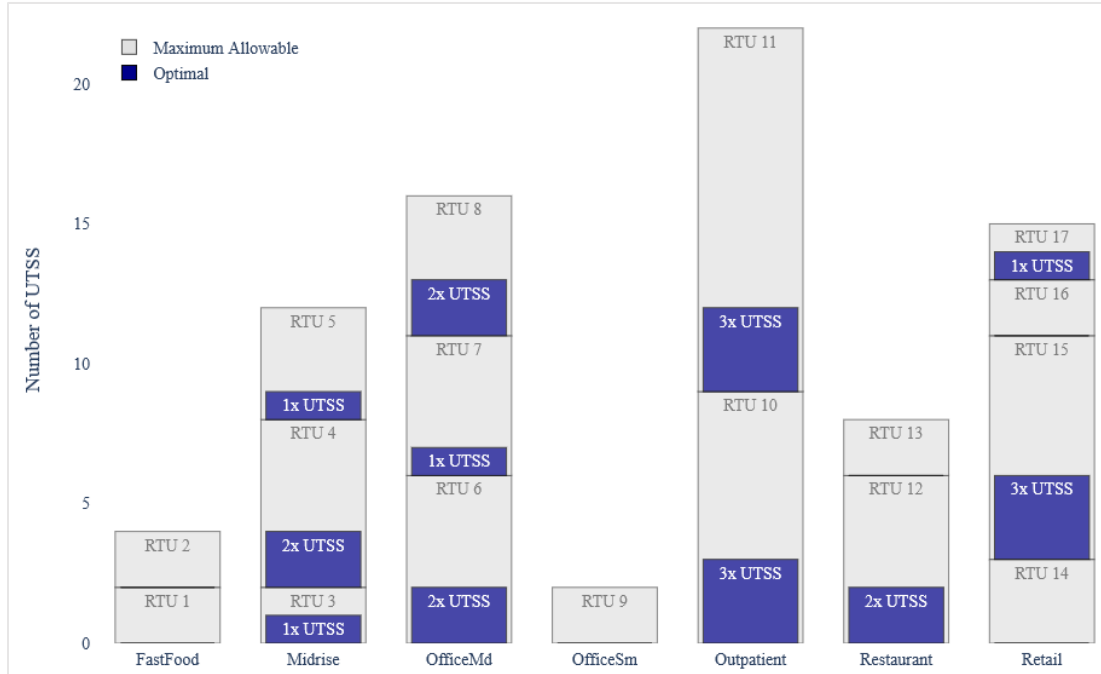


Figure 6: Optimal UTSS placement by RTU, grouped by building. Each gray box depicts the maximum number of UTSS that could be assigned to given RTU, which is equivalent to the parameter m_m . The blue boxes depict the number and location of UTSS given by the optimized solution.

4.3 Optimal Dispatch

The optimization program also provides RTU-level dispatch schedules for every UTSS within the community. Figure 7 shows the aggregate community electric demand profiles of both the baseline and optimized cases for (a) the entire annual period and (b) a selected August week. In the annual demand profile comparison, the optimization response to the monthly demand charges is illustrated through the new maximum power values, most apparent during the summer months.

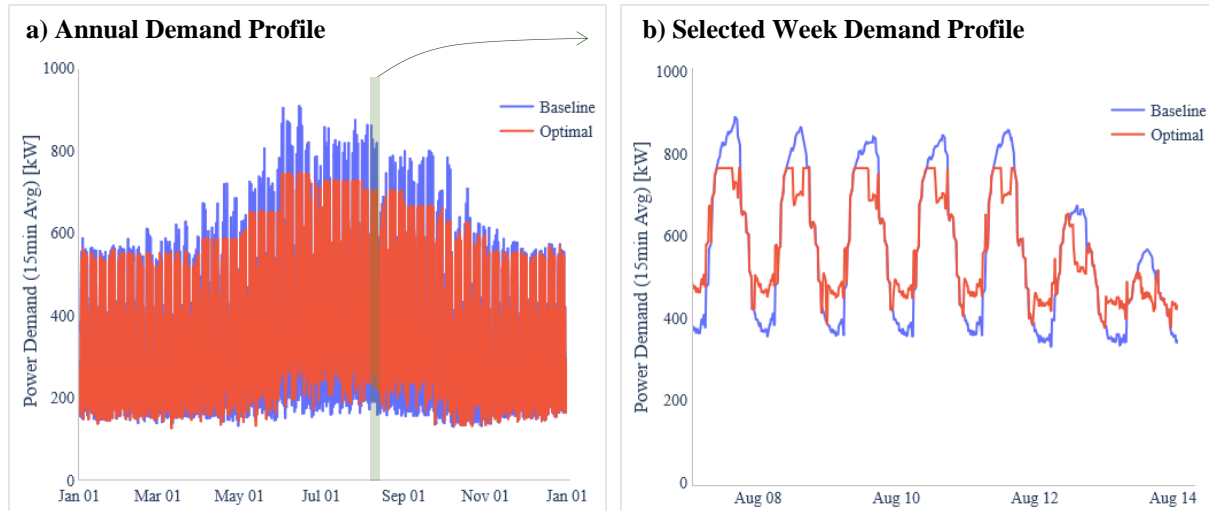


Figure 7: Comparison of Baseline and Optimal aggregated electric demand profiles. (a) shows the full-year profile, where optimized maximum values for each demand period d (one per month) are clearly visible. (b) shows one selected week, illustrating charge and discharge periods, as well as the optimization response to both demand charges and time-of-use energy charges.

The demand profile over the selected week of August 7-13 shows the daily performance of the optimized thermal storage relative to baseline. Here we see the response to both demand charges and time-of-use energy charges. Overnight charging does not immediately begin at the end of the day but occurs as late as possible. This maximizes charging efficiency as the ambient temperatures during early morning hours are typically lower than at late evening. It also minimizes thermal losses from the storage tank before the ice is used.

A load duration curve is the annual electric demand profile sorted from highest to lowest values. These curves provide a qualitative indication of the variation of the electric load over the course of the year. They also tell how much total time within the year that the load is above a certain value.

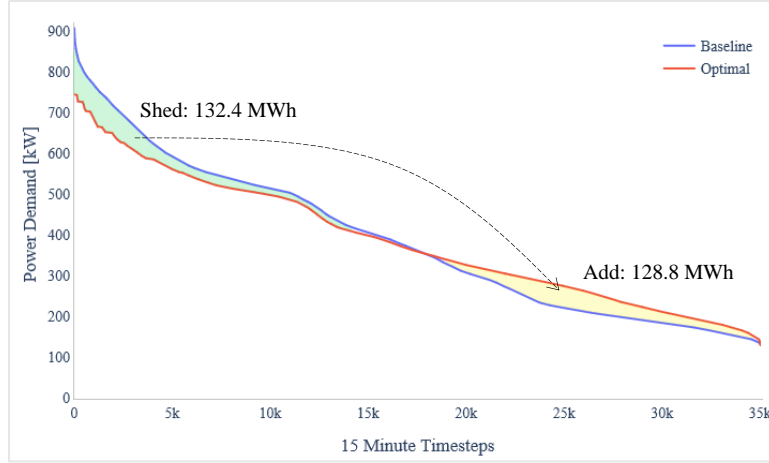


Figure 8: Annual Load duration curve for the community aggregate power demand

Figure 8 presents the load duration curves for the community aggregate electric power demand for both the baseline and optimized cases. Deployment of UTSS has a flattening effect on the curve, producing a more stable load to the electric grid. It also reduces maximum annual power demand by 165 kW_e. Load Shed (area between the curves when the optimal lies below the baseline) is 132.4 MWh while Load Add (area between the curves when the optimal falls above the baseline) is 128.8 MWh. Thus, the load shift efficiency (η_{shift}), is 1.028. This decrease in annual energy use relative to baseline is achieved by the optimized control, which charges at times of maximum efficiency, rather than following a simple schedule-based charging signal. However, η_{shift} is highly dependent on the relative efficiencies of the ice-making compressor within the UTSS and the baseline cooling equipment. It is also a function of ambient weather and building thermal zone conditions. Because our location experiences large diurnal temperature swings, conditions are favorable for off-peak ice-making. The optimization formulation is not written to maximize energy efficiency, but rather to minimize total cost. Given a different set of buildings in a different climate zone, η_{shift} may not exceed 1, especially if the electricity tariff promotes daytime ice charging.

Figure 9 shows the dispatch control signals for (a) each UTSS at its associated RTU for the whole year and for (b) the UTSS at RTUs 3 and 10 for the selected week of August 7-13. All values are normalized against the maximum rates of charging and discharging for each RTU. Positive values indicate charging; negative values indicate discharging. Individual UTSS dispatch signals reveal three insights into the charging rates, discharging rates, and seasonal importance of thermal storage. Figure 9a show all UTSS predominantly charge at the maximum

possible rate. Unlike central chiller-ice plants which experience improved efficiency when ice charging rates are limited [62], the particular characteristics of UTSS encourage charging as quickly as possible when ambient conditions are favorable.

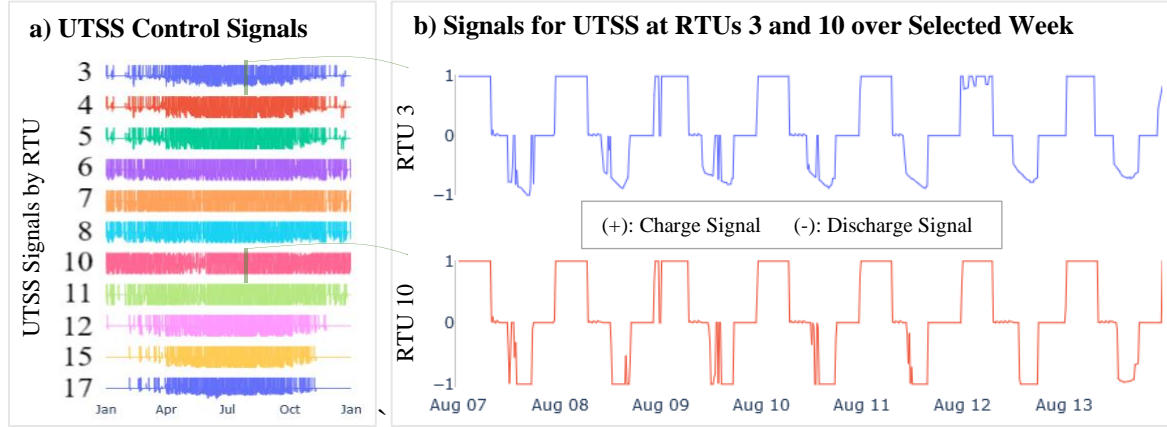


Figure 9: Control signals for each UTSS at their respective RTUs. Positive values are charging signals; negative values are discharging signals. All values are normalized against the appropriate maximum rate of heat transfer at each RTU and timestep ($Z_{1n} \cdot \bar{q}_{1n}^X$ or $Z_{1n} \cdot \bar{q}_{1n}^Y$). (a) shows all the UTSS signals for the entire year. (b) shows the dispatch signals for RTUs 3 and 10 for a selected August week.

Conversely, full-year profiles show discharging rates are often not at maximum values. Figure 9b shows UTSS at RTU 10 is discharged generally at its maximum rate, but over a narrower average daily window compared to RTU 3. The UTSS at RTU 3, which is much smaller, discharges at a limited rate over a longer period each day. An interesting observation emerges from these two examples: the larger RTU with more thermal storage is dispatched primarily during the on-peak hours of 12:00-18:00, when TOU charges are highest and peak demand occurs. The storage at the smaller RTU is dispatched more slowly over the course of the day, providing a demand shaving role during both on-peak and off-peak hours. The requisite data analysis to confirm if this dispatch trend applies generally exceeds the scope of our present study.

4.4 Sensitivity Results

4.4.1 Median UTSS State-of-Charge

Changing the assumption for median UTSS state-of-charge does not alter the integer solution, nor does it appreciably change the linear solutions for charging and discharging. Variation in the optimization result is negligible between $\tilde{\alpha}_1$ values of 0.95 and 0.05, with minimum annual cost decreasing from \$235,076 to \$234,938, or a 0.04% change. All this change

is manifest in the energy charges, with demand charges remaining constant between solutions. Furthermore, the change in energy charges is most significant at lower \tilde{s}_1 values. The total change in cost between 0.95 and 0.55, the value we used in this case study, was only \$22 annually.

However, despite the negligible impact on optimized minimum cost, we find the value of \tilde{s}_1 to be significant in determining overall system efficiency. Increasing \tilde{s}_1 from 0.55 to 0.95 results in a reduction in η_{shift} from 1.028 to 0.995. Decreasing \tilde{s}_1 from 0.55 to 0.05 results in a much higher η_{shift} of 1.14. This substantial increase in round-trip electric efficiency at lower \tilde{s}_1 occurs because the calculated maximum rates and efficiencies for charging are higher at very low states-of-charge. Thus, the optimization can charge the tank more quickly at the times of highest efficiency.

Upon close examination of the UTSS charging efficiency curve, Equation 3, we find that COP for charging decreases linearly as state-of-charge increases from 0.15 to 0.95. However, when $\tilde{s}_1 < 0.15$, charging efficiency spikes. When normalized against our demonstration case assumption of $\tilde{s}_1 = 0.55$, the relative COP varies as shown in Figure 10. So long as ice tank state-of-charge is maintained above 0.15, the efficiency for ice charging will vary by $\pm 2\%$; however, below that range, relative efficiency increases by $> 7\%$. This, compounded with the increased charging capacity associated with lower states-of-charge, explains the exceedingly high load shift efficiency value obtained when optimizing with $\tilde{s}_1 = 0.05$.

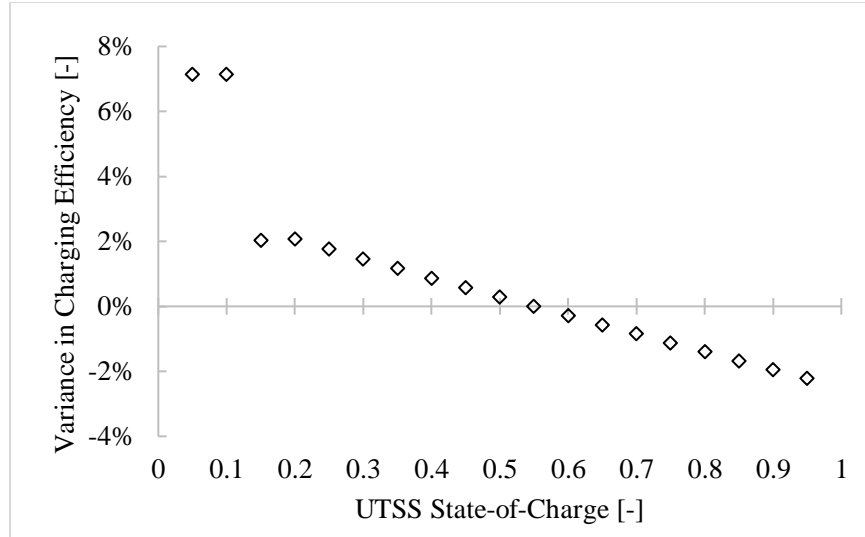


Figure 10: Variance in charging efficiency (COP_{tr}^x) as a function of ice tank state-of-charge (\tilde{s}_1), normalized against $\tilde{s}_1 = 0.55$, the value used in our demonstration optimization.

Because the impacts of the \tilde{s}_1 assumption are manifest in both charging and discharging, and off-peak energy costs are quite low, the total optimization results are essentially unchanged. However, the energy efficiency results vary significantly, especially at \tilde{s}_1 values below 0.15. In our demonstration case, we partially mitigate this by reducing each UTSS nominal capacity to a usable capacity, and benefit from the fact that most of the time the UTSS states-of-charge are well above 15%. Nevertheless, the median state-of-charge assumption is significant, and can lead to an over-estimation of the electrical efficiency of the optimal design.

4.4.2 Optimization Timestep

Table 6 shows the capacity-normalized sensitivity results calculated using different optimization timesteps, with 15-minutes as the reference case. Though the building simulation timestep remains fixed at 1-minute, as optimization timestep changes from 15 to 30 to 60 minutes, the total number of UTSS in the solution increases. Energy charges do not vary as timestep increases, but the maximum values for peak demand are somewhat reduced by the smoothing effect of the longer averaging window. This causes an increase in importance of energy charges relative to demand charges. The relative savings achieved by the optimization decreases by the values shown in Table 6. This confirms that the MILP is sensitive to the optimization timestep independent of the building energy simulation timestep, and should be set equal to the value required to accurately calculate the electricity bill.

Table 6: Comparison of results using different optimization timesteps

Optimization Timestep	Optimal Number of UTSS	Relative Change in Cost Savings
15 min	21	Reference
30 min	22	-3.1%
60 min	23	-5.6%

4.4.3 Annualized Life Cycle Cost of Storage

The parametric sweep over the full range of possible ALCC values provides insight into the potential maximum impact of using distributed UTSS within the community, and it reveals RTU prioritization for UTSS integration. Figure 11 shows the minimum annual cost results for 42 optimization runs with the ALCC (k_{in}) ranging from \$50 to \$2150 per device per year. The red dashed line is the maximum possible cost from the optimization, which is equal to the baseline annual energy bill of \$247,400. The green dashed line is the minimum possible cost if (1) all cooling electric energy is purchased at off-peak rates and dispatched assuming $\eta_{shift} = 1$, and (2) demand charges are dictated only by non-cooling loads. For our community, this value is \$180,600, which represents a 29.7% potential reduction in the total annual electric bill. As the ALCC increases, the total number of UTSS procured decreases, shown by the blue diamonds in Figure 11b. When k_{in} exceeds \$2150 per device per year, the optimization determines thermal storage to be too expensive and returns the baseline, no-storage case.

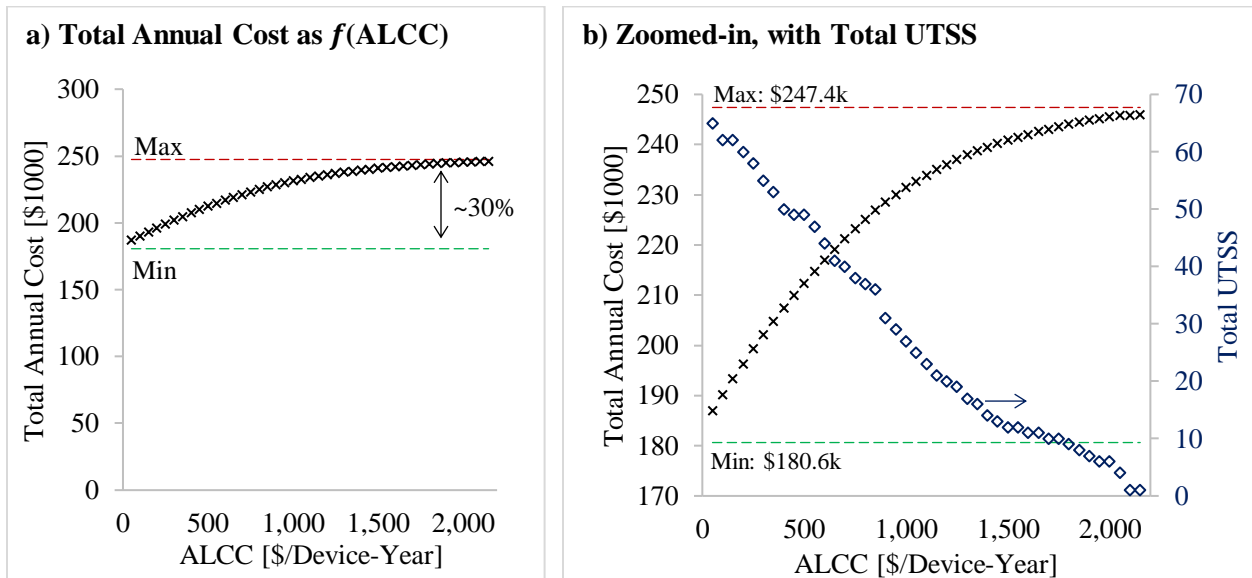


Figure 11: Optimization results as a function of ALCC, bounded by the baseline annual energy bill (Max) in red and the minimum possible energy bill (Min) in green. (a) Total annual cost shown at full scale relative to the energy bill,

illustrating a potential 29.7% savings. **(b)** Zoomed-in results with the total number of UTSS determined by the optimization plotted on the secondary axis.

This parametric sweep also provides information on the relative priority of each RTU for receiving thermal storage. Figure 12 shows the total number of UTSS procured as a function of ALCC but broken out by RTU assignment. Moving from right-to-left on Figure 12 identifies the price point at which each UTSS is added at a given RTU. For example, we see that RTU 15 (light gray, near the top) should be the first one to receive UTSS at an annualized cost of \$2,100, while RTU 16 in the same building (yellow, top) should not receive UTSS until the price drops below \$1,100 per device per year. Similarly, RTU 10 (gold, middle) should be prioritized over RTU 11 (blue, middle), even though both are in the same building and RTU 11 is larger.

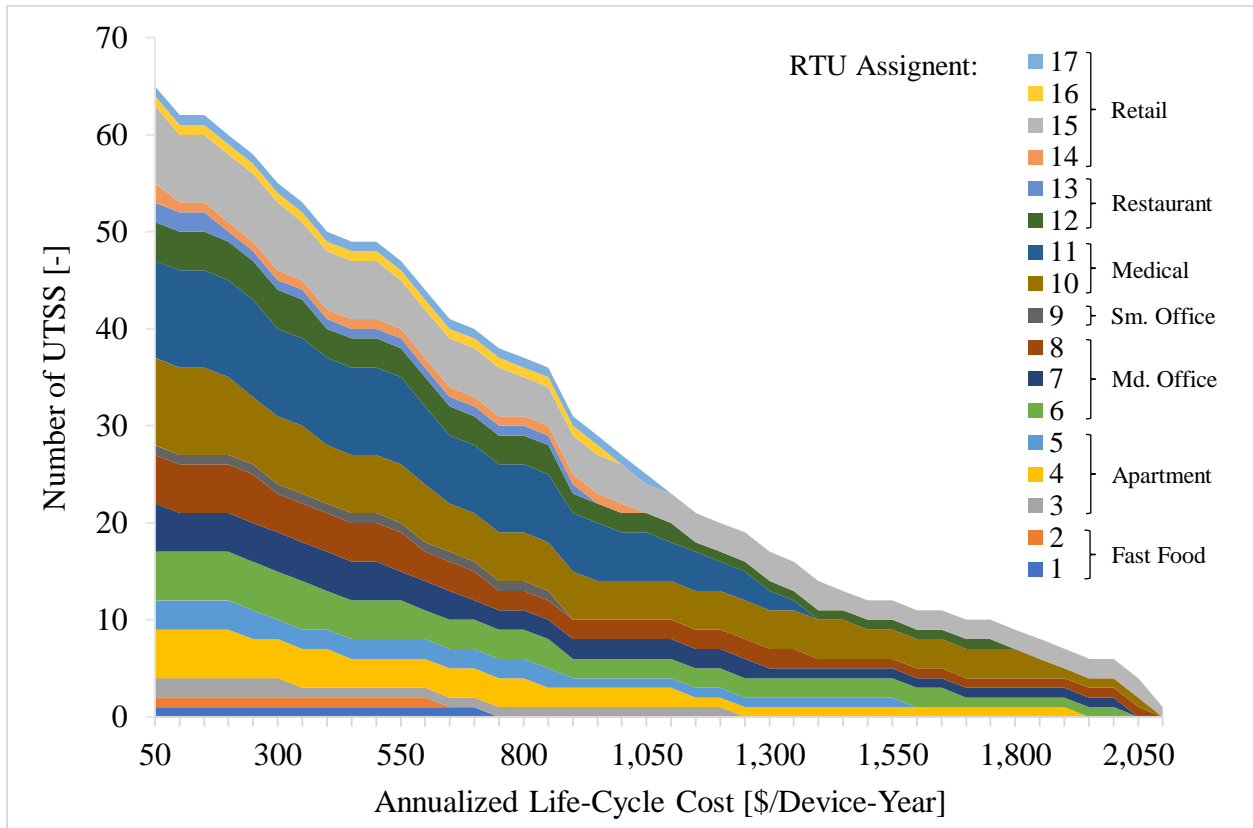


Figure 12: Total number of UTSS determined by the optimization, divided by RTU assignment, as a function of annualized life-cycle cost of the UTSS.

On a shared machine this parametric sweep of 42 complete optimization runs took approximately 63 hours using 15-minute optimization timesteps, but only 4.5 hours using 60-minute timesteps (with somewhat different results, as discussed above). As this type of analysis is strategic in scope and belongs early in a new construction or retrofit design process, we find the insight that it provides for UTSS placement priorities to be well worth the computer run time.

5. Utility of the Community Optimization Approach

This optimization workflow is designed to be highly scalable, equally applicable to a single building with a single RTU or to a multitude of buildings with many RTUs. As the community increases in size the number of variables also necessarily increases. To retain problem tractability without modifying the formulation as the problem size grows, the optimization timestep may be lengthened, with the noted loss in solution fidelity, discussed previously. Other methods, such as reducing the optimization horizon (T) from the full-year to a shorter operating season, aggregation of similar HVAC systems/loads across the community, or using a multi-step optimization which dissociates the design and dispatch aspects may also be useful; however, they are not assessed within this paper.

Considering the large size of a multi-building HVAC optimization problem, one may question the value of this aggregated approach. To demonstrate the utility of our approach, we apply the optimization individually for each of the seven buildings in our demonstration case, aggregate those individual results, and compare them with our connected community optimization. The significant differences in the results for each approach illustrate the value of our method, despite the additional computation time required by the solver.

Table 7: Comparison between community and individual building optimization approaches

Optimization Approach	Total UTSS	Baseline Annual Cost	Optimal Annual Cost	Relative Savings	Solve Time [min]
Community	21	\$247,404	\$235,054	5.0%	85
Individual Building	19	\$253,294	\$243,987	3.7%	25

Table 7 shows a few of the differences in the optimization results obtained between the two methods. It is important to note that the value of the baseline energy bill is lower for the community approach due to the difference in demand charges assessed by the two methods. Nevertheless, even though it is optimizing against a lower baseline energy bill, the community approach can capitalize on the diversity in building loads to obtain greater relative (and absolute) annual savings. If only the energy bills are considered (excluding hardware costs), the community optimization produces a savings of \$35,975 (14.5%) vs. \$30,682 (12.1%) for the aggregated individual building optimizations. The individual building approach results in fewer total UTSS installed, and it places them differently than the community approach does. RTUs 3,

6, 11, and 12 receive one fewer UTSS each; and RTUs 9 and 10 each receive one additional UTSS. This results in less overall storage placed in the Midrise Apartment, the Medium Office, and the Restaurant with the individual optimization approach. Surprisingly, the Small Office receives storage under the individual optimization, which it does not when using the community approach. While the solution time is ~ 3.5 times greater than that required for an individual building optimization approach, the community approach produces different design and dispatch results for greater cost savings.

6. Conclusions

We present a new simulation-optimization workflow that employs building energy modeling software and a mixed-integer linear program to optimally design and dispatch ice-based unitary thermal storage systems within connected communities. The workflow is modular and allows for any BEM or optimization solver to be used. The UTSS regression model is extracted from the EnergyPlus source code and placed into a separate Python script, allowing for custom tuning, should sufficient data be available. This workflow is useful in evaluating the economic potential of packaged ice storage systems within the GEB context and is scalable from a single building to large communities.

We demonstrate the workflow using a seven-building case study in El Paso, TX, with 17 RTUs at which UTSS might be placed. Using realistic electric rates and capital costs, our optimization workflow finds an optimal distribution of 21 UTSS across 11 of the available RTUs in five buildings. Annualized expenditures for the UTSS are \$23,625, but energy bill savings are \$36,045, resulting in a net annual savings of \$12,420 across the district. Cooling-only electricity costs are reduced 51.6%, excluding UTSS costs, compared to baseline through the optimized dispatch. Including the hardware costs, the cooling-only energy savings remain quite substantial at 17.8% annually.

To assess the validity of our workflow assumptions, we perform three small parametric studies. We find the median UTSS SOC parameter (\tilde{s}_i) to be insignificant in affecting the optimized design or dispatch, but it does affect any whole system efficiency calculations made during post-processing. The optimization timestep (δ) is significant, independent of the building simulation timestep, and should be set at a value adequate for accurate energy bill calculations.

We also perform a broad sweep over the full range of possible ALCC values (k_m) and examine the design results as a function of cost.

Based on the analyzed community, we conclude that the design and dispatch of UTSS at the community scale out-performs individual building optimization by taking advantage of the load diversity across multiple buildings. In our demonstration case, the optimal design produces 5% savings in the annual energy bill, after accounting for UTSS hardware costs, which compares favorably to only 3.7% savings obtained using an individual building approach. If hardware costs are excluded, the community optimization produced an annual savings of 14.5% vs. 12.1% when using an individual building approach.

Future work associated with this project includes adding a re-simulation step following the optimization to evaluate the UTSS design and dispatch signals within the building energy modeling platform. This will capture the building-specific non-linear effects that are not captured in our MILP. Additionally, this approach is based on known weather inputs, and is therefore useful for early design analysis and the development of heuristic control strategies. Additional data analysis to develop these heuristic controls for UTSS operating dynamically throughout the day should be performed. The utility of the optimization model for business-case analyses could benefit by reformulating the objective to be a function of required payback period instead of annualized capital cost. Finally, future analyses would benefit from more thoroughly validated UTSS models, especially ones that capture partial charge/discharge operation. We hope that our workflow provides a useful starting place in helping answer how packaged cool thermal storage should be distributed and controlled in the GEB future.

Acknowledgements

We would like to acknowledge the National Renewable Energy Laboratory for funding this research through the Alliance Partner University Program contract number UGA-0-41025-152. We would also like to thank Dr. Alexandra Newman of Colorado School of Mines for her contributions to improve our optimization program formulation.

References

[1] Bowers R. Updated Renewable Portfolio Standards Will Lead to More Renewable Electricity Generation. Today in Energy: U.S. Energy Information Administration (EIA); 2019.

- [2] Neukomm M, Nubbe V, Fares R. Overview of Research Challenges and Gaps. Grid-Interactive Efficient Buildings Technical Report Series: U.S. Department of Energy Office of Energy Efficiency and Renewable Energy; 2019. p. 44.
- [3] Metrics for Building Demand Flexibility (Draft). Lawrence Berkeley National Lab; 2019. p. 2.
- [4] Lanahan M, Engert S, Kim T, Tabares-Velasco PC. Rapid Visualization of the Potential Residential Cost Savings from Energy Storage Under Time-of-Use Electric Rates. *Journal of Building Performance Simulation*. 2019;12:68-81.
- [5] Chen Y, Xu P, Gu J, Schmidt F, Li W. Measures to Improve Energy Demand Flexibility in Buildings for Demand Response (DR): A Review. *Energy and Buildings*. 2018;177:125-39.
- [6] Song X, Liu L, Zhu T, Chen S, Cao Z. Study of Economic Feasibility of a Compound Cool Thermal Storage System Combining Chilled Water Storage and Ice Storage. *Applied Thermal Engineering*. 2018;133:613-21.
- [7] Song X, Zhu T, Liu L, Cao Z. Study on Optimal Ice Storage Capacity of Ice Thermal Storage System and Its Influence Factors. *Energy Conversion and Management*. 2018;164:288-300.
- [8] Fact Sheet: Grid-interactive Efficient Buildings. Washington, D.C.: U.S. Department of Energy Office of Energy Efficiency and Renewable Energy; 2019. p. 2.
- [9] Glazer J. ASHRAE Design Guide for Cool Thermal Storage. 2nd ed 2019. p. 312.
- [10] Taylor RD. Development of an Integrated Building Energy Simulation with Optimal Central Plant Control [Dissertation]. Ann Arbor: University of Illinois at Urbana-Champaign; 1996.
- [11] MacCracken MM. Thermal Energy Storage Myths. *ASHRAE Journal*. 2003;45.
- [12] Chaichana C, Charters WWS, Aye L. An Ice Thermal Storage Computer Model. *Applied Thermal Engineering*. 2001;21:1769-78.
- [13] Ruan Y, Liu Q, Li Z, Wu J. Optimization and Analysis of Building Combined Cooling, Heating and Power (BCHP) Plants with Chilled Ice Thermal Storage System. *Applied Energy*. 2016;179:738-54.
- [14] Monsef H, Yari M. Design and Analysis of an Ice Thermal Storage System for Residential Air-Conditioning Applications. *International Journal of Exergy*. 2016;20:122-38.
- [15] Kamal R, Moloney F, Wickramaratne C, Narasimhan A, Goswami DY. Strategic Control and Cost Optimization of Thermal Energy Storage in Buildings Using EnergyPlus. *Applied Energy*. 2019;246:77-90.
- [16] Van Asselt A. Model Predictive Control of Cool Thermal Energy Storage Under Different Electricity Rate Structures. 2019 ASHRAE Annual Conference. Kansas City, MO: ASHRAE; 2019. p. 8.
- [17] Henze G. Evaluation of Optimal Control for Ice Storage Systems [Dissertation]. Ann Arbor, MI: University of Colorado; 1995.
- [18] Augusto GL, Culaba AB, Maglaya AB. Identification of Design Criteria for District Cooling Distribution Network with Ice Thermal Energy Storage System. *Energy Procedia*. 2015;79:233-8.
- [19] Mazzoni S, Sze JY, Nastasi B, Ooi S, Desideri U, Romagnoli A. A Techno-Economic Assessment on the Adoption of Latent Heat Thermal Energy Storage Systems for District Cooling Optimal Dispatch & Operations. *Applied Energy*. 2021;289:116646.
- [20] Massie DD. Optimal Neural Network-Based Controller for Ice Storage Systems [Dissertation]. Ann Arbor: University of Colorado at Boulder; 1998.
- [21] Cox SJ, Kim D, Cho H, Mago P. Real Time Optimal Control of District Cooling System with Thermal Energy Storage Using Neural Networks. *Applied Energy*. 2019;238:466-80.

- [22] Al Rifaie FHZ. An Integrated Approach to Optimally Design and Operate Ice Thermal Storage for Typical HVAC Systems [Dissertation]. Ann Arbor: North Carolina Agricultural and Technical State University; 2017.
- [23] Sanaye S, Shirazi A. Four E Analysis and Multi-Objective Optimization of an Ice Thermal Energy Storage for Air-Conditioning Applications. *International Journal of Refrigeration*. 2013;36:828-41.
- [24] Chavez P, Stingelin D. Thermal Energy Storage New Mexico State University. Rocky Mountain APPA; 2019.
- [25] IceBank Energy Storage Installations. 2020.
- [26] Naranjo Palacio S, Valentine KF, Wong M, Zhang KM. Reducing Power System Costs with Thermal Energy Storage. *Applied Energy*. 2014;129:228-37.
- [27] Van Asselt A, Reindl D, Nellis G, Klein S. Design and Utilization of Thermal Energy Storage to Increase the Ability of Power Systems to Support Renewable Energy Resources. 2017. p. 174.
- [28] Hao L, Wei M, Xu F, Yang X, Meng J, Song P, et al. Study of Operation Strategies for Integrating Ice-Storage District Cooling Systems into Power Dispatch for Large-Scale Hydropower Utilization. *Applied Energy*. 2020;261:114477.
- [29] Commercial Building Energy Consumption Survey (CBECS). U.S. Energy Information Administration (EIA); 2012.
- [30] AHRI. Performance Rating of Thermal Storage Equipment Used for Cooling. Arlington, VA: AHRI; 2014. p. 68.
- [31] NETEnergy Partnerships. NETEnergy; 2019.
- [32] Jones AT, Finn DP. Co-Simulation of a HVAC System-Integrated Phase Change Material Thermal Storage Unit. *Journal of Building Performance Simulation*. 2017;10:313-25.
- [33] Hunt E. Ice Energy Completes First Phase of Largest Distributed Thermal Storage System Installation in U.S. 2019.
- [34] Spector J. Ice Energy, Thermal Storage Evangelist, Files for Bankruptcy. *Greentech Media*; 2020.
- [35] Kung F, Deru M, Bonnema E. Evaluation Framework and Analyses for Thermal Energy Storage Integrated with Packaged Air Conditioning. 2013. p. 102.
- [36] EnergyPlus. 9.3.0 ed: U.S. Department of Energy; 2020.
- [37] Heine K, Tabares-Velasco PC, Deru M. Energy and Cost Assessment of Packaged Ice Energy Storage Implementations Using OpenStudio Measures. *Energy and Buildings*. (Under Review).
- [38] Barbour E, Parra D, Awwad Z, González MC. Community Energy Storage: A Smart Choice for the Smart Grid? *Applied Energy*. 2018;212:489-97.
- [39] Jones EC, Leibowicz BD. Co-Optimization and Community: Maximizing the Benefits of Distributed Electricity and Water Technologies. *Sustainable Cities and Society*. 2021;64:102515.
- [40] Cole WJ. Dynamic modeling, optimization, and control of integrated energy systems in a smart grid environment 2014.
- [41] Cole WJ, Rhodes JD, Gorman W, Perez KX, Webber ME, Edgar TF. Community-scale residential air conditioning control for effective grid management. *Applied Energy*. 2014;130:428-36.
- [42] REopt Capabilities. National Renewable Energy Laboratory; 2020.
- [43] URBANopt SDK Documentation. National Renewable Energy Laboratory; 2021.
- [44] Xendee. Home - XENDEE Microgrid Design Platform. 2020.

- [45] HOMER - Hybrid Renewable and Distributed Generation System Design Software. 2021.
- [46] Heine K, Tabares-Velasco PC, Deru M, Polly B. Quantifying the Value of Unitary Thermal Energy Storage Systems (UTSS): A Modelling Study. *Building Simulation* 19. Rome, Italy: IBPSA; 2019.
- [47] DER-CAM | Grid Integration Group. Lawrence Berkeley National Laboratory; 2020.
- [48] Christians M. In: Tabares-Velasco PC, editor. *Email Correspondence* ed2020. p. 2.
- [49] Weather Data | EnergyPlus. U.S. Department of Energy; 2020.
- [50] Commercial Prototype Building Models | Building Energy Codes Program. U.S. Department of Energy; 2020.
- [51] Goldwasser D, Long N. *openstudio-common-measures-gem*. 0.2.0 ed: National Renewable Energy Laboratory; 2020.
- [52] Parker A, Yixing Chen Y, Adams M, Sun K, Maholtra M, Goldwasser D, et al. *openstudio-standards*. 0.2.11 ed: National Renewable Energy Laboratory; 2020.
- [53] Electric EP. *Electricity for West Texas and Southern New Mexico | El Paso Electric | Texas Rate Tariffs*. El Paso Electric; 2020.
- [54] Parsonnet B, Willis Jr. RR, Wiersma DL. System and Method for Liquid-Suction Heat Exchange Thermal Energy Storage. In: Office USPaT, editor.: Ice Energy Inc; 2013.
- [55] Narayanamurthy R. Thermal Energy Storage and Cooling System with Secondary Refrigerant Isolation In: Office USPaT, editor. F25D 3/00 (20060101) ed: Ice Energy Holdings, Inc.; 2010.
- [56] Tan P, Lindberg P, Eichler K, Löveryd P, Johansson P, Kalagasidis AS. Thermal Energy Storage Using Phase Change Materials: Techno-Economic Evaluation of a Cold Storage Installation in an Office Building. *Applied Energy*. 2020;276:115433.
- [57] Database of State Incentives for Renewables & Efficiency® - DSIRE. N.C. Clean Energy Technology Center; 2019.
- [58] Benders JF. Partitioning Procedures for Solving Mixed-Variables Programming Problems. *Numerische Mathematik*. 1962;4:238-52.
- [59] IBM ILOG CPLEX Optimization Studio v.12.10: Benders algorithm. IBM; 2014.
- [60] Good N, Zhang L, Navarro-Espinosa A, Mancarella P. High Resolution Modelling of Multi-Energy Domestic Demand Profiles. *Applied Energy*. 2015;137:193-210.
- [61] Lu S, Gu W, Zhou S, Yu W, Yao S, Pan G. High-Resolution Modeling and Decentralized Dispatch of Heat and Electricity Integrated Energy System. *IEEE Transactions on Sustainable Energy*. 2020;11:1451-63.
- [62] Henze GP, Krarti M, Brandemuehl MJ. Guidelines for Improved Performance of Ice Storage Systems. *Energy and Buildings*. 2003;35:111-27.